

ROLE OF NUMERICAL SIMULATIONS IN THE SELECTION OF THE BEST MULTI STEP FORGING TECHNOLOGY

ŁUKASZ BĄCAL^{1*}, MARIUSZ SKÓRA²

¹ AGH Akademia Górniczo-Hutnicza, Department of Applied Computer Science and Modelling,
al. Mickiewicza 30, 30-059 Kraków

² KOELNER Łańcucka Fabryka Śrub Spółka z o.o., Poland

*Corresponding author: lukii1987@gmail.com

Abstract

Application of numerical simulations to the evaluation of the manufacturing cycle for connecting parts is the objective of the paper. The cycle is composed of rod drawing and multi step forging. Two technological variants of manufacturing part were considered. Such aspects as tool wear and possibility of changing die shape to improve its wear resistance were investigated. The better variant was selected.

Key words: numerical simulation, computer aided design, forging, connecting parts

1. INTRODUCTION

Numerical simulations help to predict behaviour of the material during plastic deformation. Forging process has several centuries tradition, while the theory of plasticity is relatively young scientific discipline. This theory, however, allows to understand better the forging process. Numerical simulations, which are based on the theory of plasticity and numerical methods, are an efficient tool, which helps design of the best forging technology (Kuziak et al., 1994; Kuziak et al., 2011a; 2011b). Not only one step forming operations are considered in these analyses, but also whole manufacturing chains are simulated (Pietrzyk et al., 2008; Pietrzyk et al., 2010; Bariani et al., 2011). Application of the finite element simulation code to the design of multi step forging of fasteners is the subject of the present work.

Fast development of the finite element simulation method was observed during last few decades.

In 1990s of the last century the FE programs were combined with model of microstructure evolution and tool wear and fracture criteria were implemented in these programs. In consequence, solution of various complex problems in the design of the forging technology became possible. Improvement of the forging of fasteners with the tool life selected as the main optimization criterion was the objective of the present work. Tool life is one of the main factors, which influence the manufacturing costs.

2. MODELS

2.1. Finite element program

Forge 3 finite element software was used in all simulations. This software is based on the Norton-Hoff viscoplastic flow rule. His rule was originally introduced by Norton (1929) for one-dimensional creep. It was extended by Hoff (1954) to three dimensions. The main equation of this law is:

$$\sigma = 2K \left(\sqrt{3} \dot{\epsilon}_i \right)^{m-1} \dot{\epsilon} \quad (1)$$

where: σ , $\dot{\epsilon}$ - stress and strain rate tensor, respectively, $\dot{\epsilon}_i$ - effective strain rate, K - material consistency, m - coefficient equal 1 for Newtonian fluids and 0 for rigid-plastic materials, which obey Huber-Mises yield criterion ($\sigma_f = \sqrt{3}K$) and Levy-Mises flow rule. For typical metal forming processes the values of m are in the range [0,1].

Detailed description of the model used in the Forge 3 software can be found in (Chenot & Bellet, 1992). The mechanical model is coupled with the finite element solution of the Fourier heat transport equation:

$$\nabla \cdot k \nabla T + Q = \rho c_p \frac{\partial T}{\partial t} \quad (2)$$

where: k - heat conductivity, T - temperature, Q - rate of heat generation due to plastic work, ρ - density, c_p - specific heat, t - time.

Neumann boundary condition is assumed, with the heat transfer coefficient of 10000 W/m²K at the contact surface between the tool and the forging. Cooling in air is simulated on the remaining part of the surface. Friction coefficient of 0.02 is used.

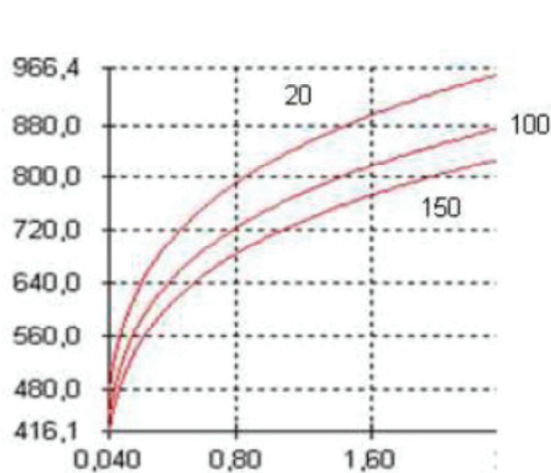


Fig. 1. The influence of temperature(left) and the strain rate (right) on the flow stress.

2.2. Flow stress model

Low carbon steel 19MnB4 with the chemical composition given in table 1 was investigated. Axisymmetric compression tests were performed to determine the flow stress model of this steel. The tests were performed on the Gleeble 3800 in the Institute for Ferrous Metallurgy in Gliwice, Poland. The samples were compressed at temperatures 20-300°C and at strain rates 0.01-500 s⁻¹. The Hansel

and Spittel (1979) equation was used to describe flow stress dependence on temperature, strain and strain rate:

$$\sigma_f = A \exp(m_1 T) \epsilon^{m_2} \dot{\epsilon}^{m_3} \exp\left(\frac{m_4}{\epsilon}\right) \quad (3)$$

where: A - hardening coefficient, m_1 - temperature sensitivity, m_2 - strain sensitivity, m_3 - strain rate sensitivity, m_4 - coefficient accounting for softening during deformation.

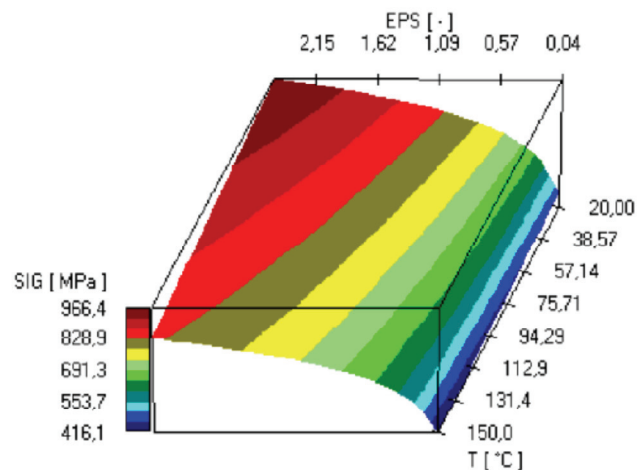
Flow stress σ_f is a material parameter in the Norton-Hoff viscoplastic model. Inverse algorithm described by Szeliga et al. (2006) was applied for identification of the coefficients in the flow stress equation (3) and the results are given in table 2.

Table 1. Chemical composition of the steel 19MnB4, wght %.

	C	Mn	Si	P	S	B
19MnB4	0.2	1.05	0.4	0.035	0.035	0.02

Table 2. Coefficients in equation (3) determined using the inverse analysis of plastometric tests.

	A	m ₁	m ₂	m ₃	m ₄
19MnB4	841.17	-0.00112	0.17546	0.01271	0.00116



Low values of coefficients m_1 , m_3 and m_4 in equation (3) mean that temperature sensitivity and strain rate sensitivity are low and softening during deformation is negligible (figure 1).

2.3. Tool wear

An increased tool life is required for economical production with high process reliability. Therefore, estimation of the tool life was included in the pro-



cess of the design of the manufacturing cycle. Depending on the temperature of the process and the tool velocity, various mechanisms of the tool failure are possible (Basquin, O.H., 1910). Three tool wear models are considered in the present project. Two of them are based on the fundamental work of Archard (1953). Following the classification by Stahlberg and Hallstrom (1999), the volume of the worn off material is proportional to the sliding distance:

$$V = \frac{C_s}{H} \int_0^t p \Delta v dt \quad (4)$$

where: C_s – coefficient, H – hardness of the tool material, p – normal pressure, μ – friction coefficient, Δv – slip velocity between the die and the deformed material.

numbers in the following figures showing die wear can be used for comparison only.

3. NUMERICAL SIMULATIONS

Simulations were performed using Forge 3 software with the flow stress model given by equation (3) with coefficients in table 2. Multi step forging of the screw M6x14 was investigated. Two technological variants presented in figure 2 were considered. The difference between the first and the second technological variant is modification of shape in the 3rd stage of forging. Comparison of the tool wear in these two variants was the objective of the research (figure 2). Possibility of changing die shape was investigated.

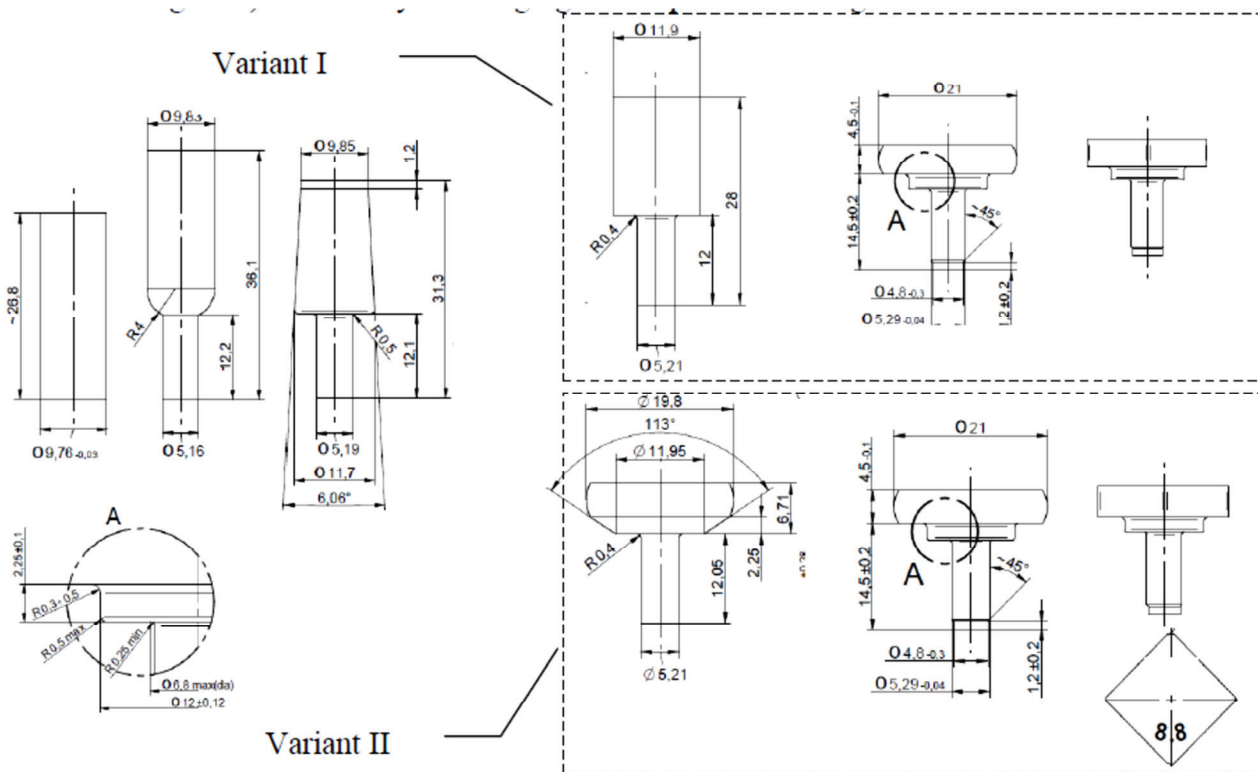


Fig. 2. Technology of manufacturing of the M6 screw – variant I and variant II.

Sliding wear is the dominant phenomenon that controls tool wear during drawing and forging in the manufacturing chain for fasteners, which is considered in the present work. The primary results of the analysis of the tool wear in the process of manufacturing of fasteners can be found in (Madej et al., 2009). In the present work various technological variants were analyzed and compared with respect to the tool wear. Since the comparison between two variants was the objective of the work, the value of the coefficient C_s was assumed as $1.2 \cdot 10^7$. Thus, the

3.1. Comparison of the two variants

Drawing is the first forming operation in the cycle. Parameters of drawing and of the first and the second stage of forging are the same for both variants. Two initial diameters of the wire were considered: 10 mm and 12 mm. Distributions of strains for these two diameters are shown in figure 3. As expected, larger strains occur for 12 mm diameter (figure 3b).



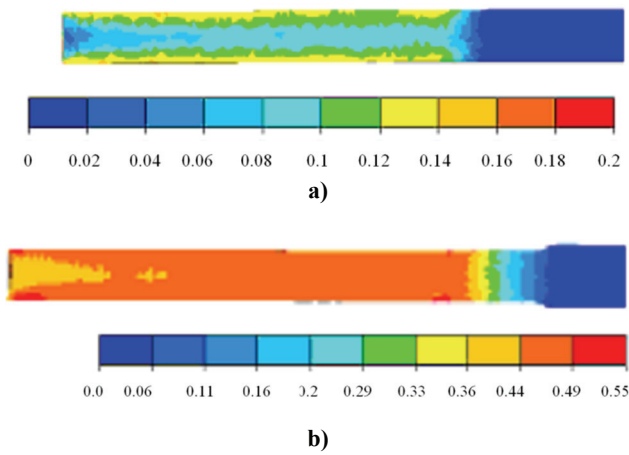


Fig. 3. Distribution of strains for the initial diameter of 10 mm (a) and 12 mm (b).

Die wear was investigated next and the results are shown in figure 4. The wear has local character when 10 mm diameter wire was drawn. Contrary, large area of wear is observed for the 12 mm diameter, but the depth of the wear is slightly lower. Larger entry diameter causes larger hardening of the material. This leads to larger tool wear during further forging operations. For this reason the diameter of 10 mm was selected for further analyses.

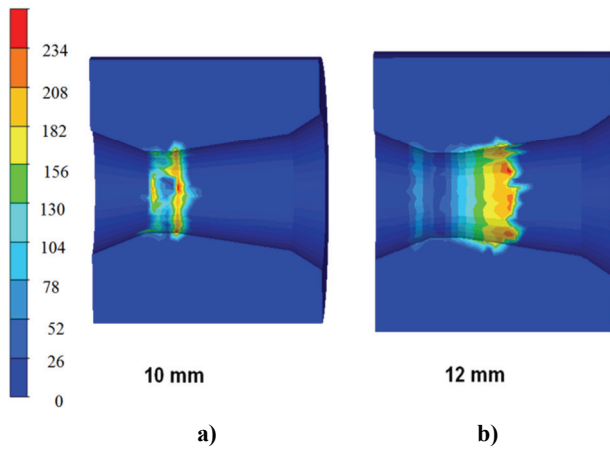


Fig. 4. Distribution of tool wear coefficient for the wire entry diameter of 10 and 12 mm.

Forging was investigated next. This process is composed of five stages, which are discussed below. First stage of forging, in which material is extruded, involves change of the wire diameter in the lower part of the screw from 9.76 mm to 5.16 mm. Strain and stress distributions at the cross section in this operation are shown in figure 5a,c. It is seen that strain concentrations occur in the area, where the largest reduction of the diameter occurs. The largest tool wear is observed in this area, as well (figure 6a). Upsetting is the main operation in the second stage of forming. Tool wear during upsetting is noticeably

lower comparing to the first stage of forging. It is due to the fact that the product diameter does not change in the second stage. The largest strain in the second stage is predicted in the location, where diameter of the screw increases from 9.83 mm to 11.7 mm (figure 5b,d). This change appears in the place, where there is no contact between the die and the workpiece (die diameter is larger than the workpiece diameter), and it has no influence on the tool wear (figure 6b).

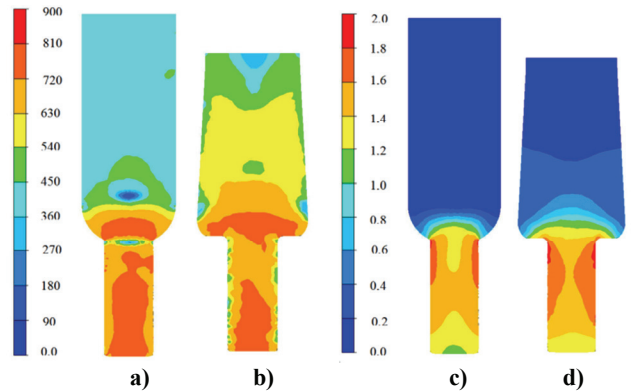


Fig. 5. Distribution of stresses [MPa] and strains after first stage of forging at the cross section: a) effective stress after first stage of forging, b) effective stress after second stage of forging, c) effective strains after first stage of forging, d) effective strains after second stage of forging.

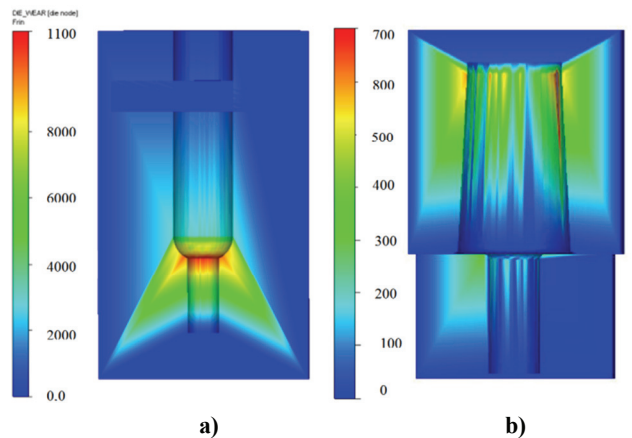


Fig. 6. Distribution of the wear coefficient according to the Archard (1953) model in the a) first stage of forging, b) second stage of forging.

In the third stage of forging the largest strain occurs in the lower part of the die. Since there is the difference between the die and the screw diameters (figure 7,8), material has to fill this part and the contact between the die and the workpiece is the longest in that area (figure 8). After completion of the first and the second variant it can be determined that the first technology is favourable as the smaller strain occurs (figure 7c,d). The tool wear is comparable for both variants. The level of intensity of deformation and the heterogeneity on the cross-section is disad-



vantageous for the second variant, which is important as analyzed operation is the initial operation before final formation of the shape of the head and the jog under the head.

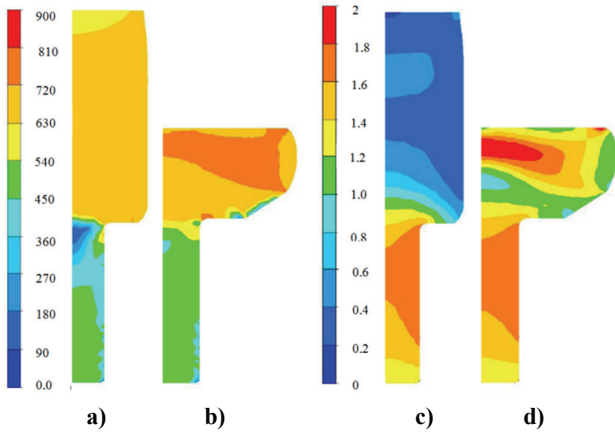


Fig. 7. Distribution of strains and stress after third stage of forging, a) effective stress distributions at the cross section for variant I, b) effective stress distributions at the cross section for variant II, c) effective strain distributions at the cross section for variant I, d) effective strain distributions at the cross section for variant II.

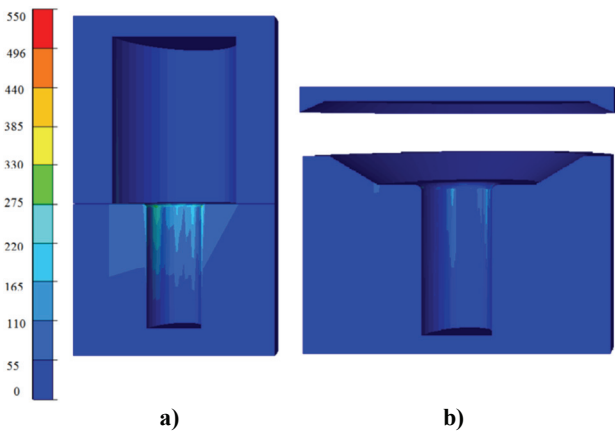


Fig. 8. Distribution of the wear coefficient according to the Archard (1953) model in the third stage of forging a) variant I b) variant II.

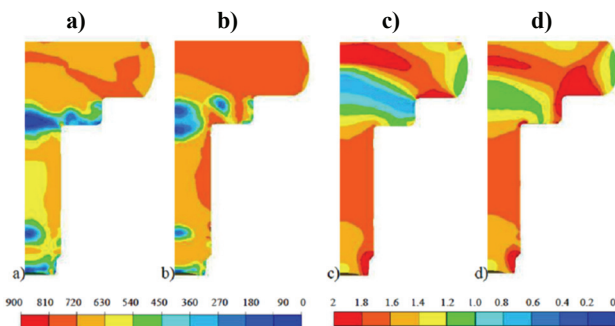


Fig. 9. Distribution of strains and stress after fourth stage of forging, a) effective stress distributions at the cross section for variant I, b) effective stress distributions at the cross section for variant II, c) effective strain distributions at the cross section for variant I, d) effective strain distributions at the cross section for variant II.

Shaping of the screw is conducted in the fourth stage of forging. Strain and stress distributions in this stage are shown in figure 9 and calculated tool wear is shown in figure 10. In the first technological variant the largest tool wear occurs in the area, where the diameter of the die changes. In the remaining part, where the diameter is constant, wear of the lower die is smaller (figure 10). The largest strains are consequently observed in the area where the diameter changes from the larger to the smaller, as well as in the head of the screw (figure 9). The noticeably higher level of the strain in the area of bearing face and the central part of the head is important for the analysis. The first variant is favourable in this stage both in terms of tool wear and the level of strains, that occur in second variant.

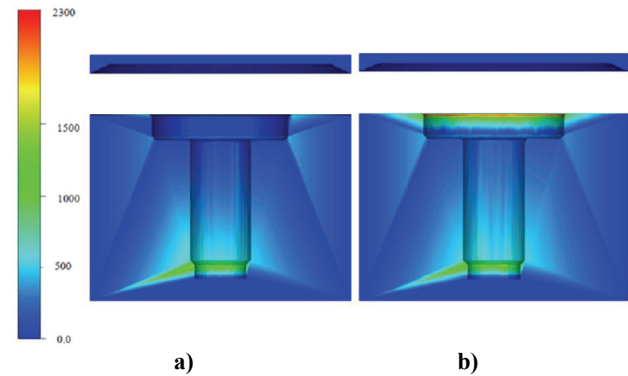


Fig. 10. Distribution of the wear coefficient according to the Archard (1953) model in the fourth stage of forging a) variant I b) variant II.

In the last stage of forging the largest concentration of strains is observed in the area, where the flash is cut off from the screw (figures 11 and 12). It is seen in figure 13 that the most intensive tool wear occurs close to the notch in the die. This fact results from the strains that emerged in multistage forging process and the accumulation of strains in the area of bearing face and in the area of free forging in the fourth operation.

Table 3. Tool wear coefficient in subsequent stages of forming for the two technological variants.

Stage	1	2	3	4	5
Variant I	11000	700	275	1250	80
Variant II	11000	700	220	2300	190

Comparison of both variants in the last stage of the whole process shows that the first variant is favorable, as the tool wear for this variant is smaller. Tool wear coefficients calculated from equation (4) for all stages of forging and for both technological



variants are given in table 3. These coefficients do not represent any physical amount of the tool wear and they should be used for comparison of various technologies only.

4. CONCLUSIONS

Drawing with lower wire entry diameter (10 mm) gives smaller strains and smaller hardening of the material. In consequence, the tool wear during following forging is smaller.

Tool wear in forging is the largest in the first stage. It decreases rapidly in the following stages, because changes of the screw diameter in these stages are small.

In the third stage of forging, where shape of dies changes, tool wear is comparable for both variants. In this stage strains and stresses are relatively high, what may cause cracks in the material and influence properties of products.

In the fourth stage of forming the variant I is better for both low tool wear and lower level of strains and stresses.

Analysis of simulations of all stages of forming allows to conclude that variant I has better parameters regarding tool wear and the level of strains and stresses.

REFERENCES

- Archard, J.F., 1953, Contact and rubbing of flat surfaces, *J. Applied Physics*, 24, 981-988.
- Bariani, P.F., Bruschi, S., Ghiotti, A., Simionato, M., 2011, Ductile fracture prediction in cold forging process chains, *CIRP Annals - Manufacturing Technology*, 60, 287-290.
- Basquin, O.H., 1910, An energy based approach to the simulation of fatigue crack initiation in metal forming tools, *Proc. ASTM*, 10, 625-630.
- Chenot, J.-L., Bellet, M., 1992, The Viscoplastic Approach for the Finite-Element Modelling of Metal Forming Processes, *Numerical Modelling of Material Deformation Processes*, eds, Hartley, P., Pillinger, I., Sturges, C.E.N., Springer-Verlag, London, Berlin, 179-224.
- Hoff, N.J., 1954, Approximate Analysis of Structures in the Presence of Moderately Large Steps Deformation, *Quart., Appl. Mech.*, 2, 49.

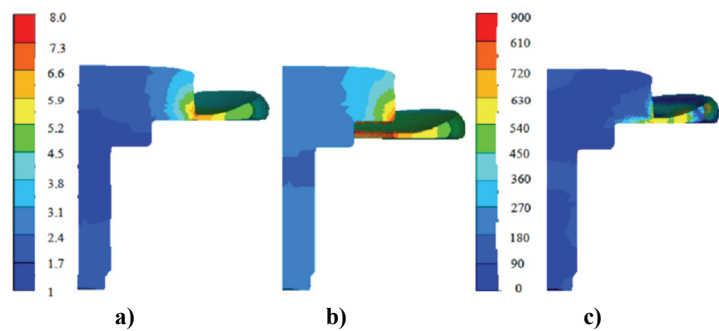


Fig. 11. Distribution of strains and stress in the fifth stage of forging variant I, a) strains before cut off flash, b) strains after cut off flash, c) stress after cut off flash.

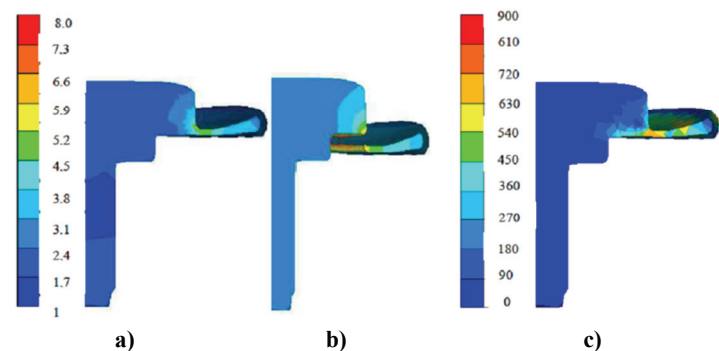


Fig. 12. Distribution of strains and stress in the fifth stage of forging variant II, a) strains before cut off flash, b) strains after cut off flash, c) stress after cut off flash.

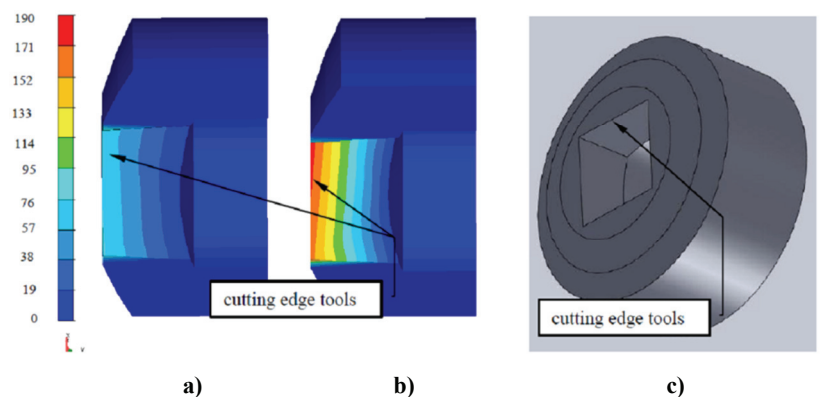


Fig. 13. Distribution of the wear coefficient according to the Archard (1953) model in the fifth stage of forging: a) variant I b) variant II, c) view of the cutting die.

- Kuziak, J., Pietrzyk, M., Chenot, J.-L., 1994, Die shape design and evaluation of microstructure control in the closed-die axis-symmetrical forging by using FORGE2 program, *ISIJ International*, 34, 755-760.
- Kuziak, R., Skóra, M., Węglarczyk, S., Paćko, M., Pietrzyk, M., 2011a, Computer aided design of the manufacturing chain for fasteners, *Computer Methods in Materials Science*, 11, 243-250.
- Kuziak, R., Pidvysots'kyy, V., Węglarczyk, S., Pietrzyk, M., 2011b, Bainitic steels as alternative for conventional carbon-manganese steels in manufacturing of fasteners - simulation of production chain, *Computer Methods in Materials Science*, 11, 443-462.



- Madej, Ł., Węglarczyk, S., Pietrzyk, M., 2009, Influence of technological parameters of manufacturing chain for steel bolts on die wear, *Hutnik-Wiadomości Hutnicze*, 76, 620-622.
- Norton, F.H., 1929, *Creep of Steel at High Temperature*, McGraw Hill, New York.
- Pietrzyk, M., Madej, Ł., Węglarczyk, S., 2008, Tool for optimal design of manufacturing chain based on metal forming, *Annals of the CIRP*, 309-312.
- Pietrzyk, M., Madej, Ł., Kuziak, R., 2010, Optimal design of manufacturing chain based on forging for copper alloys, with product properties being the objective function, *Annals of the CIRP*, 59, 319-322.
- Stahlberg, U., Hallstrom, J., 1999, A comparison between two wear models, *Journal of Materials Processing Technology*, 87, 223-229.

ROLA NUMERYCZNEJ SYMULACJI W DOBORZE NAJLEPSZEGO WARIANTU TECHNOLOGICZNEGO DLA WIELOETAPOWEGO PROCESU KUCIA

Streszczenie

Celem pracy było zastosowanie numerycznych symulacji do oceny cyklu wytwarzania elementów złącznych. Ten cykl składał się z ciągnięcia prętów oraz z pięciu etapów kucia na zimno. Rozważono dwa warianty technologii. Oceniano takie aspekty procesu jak zużycie narzędzi oraz możliwość zmian kształtu narzędzi dla poprawy ich odporności na zużycie. Na podstawie przeprowadzonych badań wybrano lepszy wariant technologiczny.

Received: February 06, 2012
Received in a revised form: April 24, 2012
Accepted: June 20, 2012

